



## A robust increase in the eddy length scale in the simulation of future climates

J. Kidston,<sup>1,2,3,4</sup> S. M. Dean,<sup>5</sup> J. A. Renwick,<sup>5</sup> and G. K. Vallis<sup>1,2</sup>

Received 30 October 2009; revised 30 November 2009; accepted 7 December 2009; published 6 February 2010.

[1] Output from the Coupled Model Intercomparison Phase 3 are analysed. It is shown that for the ‘A2’ business as usual scenario, every model exhibits an increase in the eddy length scale in the future compared with the simulation of 20th Century climate. The increase in length scale is on the order of 5% by the end of the 21st century, and the Southern Hemisphere exhibits a larger increase than the Northern Hemisphere. The inter-model variability in the increase in the eddy length scale is correlated with the variability in the increase in dry static stability at 700 hPa. Inspection of the NCEP/NCAR reanalysis data indicates that the eddy length scale in the Southern Hemisphere may have increased in recent decades. **Citation:** Kidston, J., S. M. Dean, J. A. Renwick, and G. K. Vallis (2010), A robust increase in the eddy length scale in the simulation of future climates, *Geophys. Res. Lett.*, 37, L03806, doi:10.1029/2009GL041615.

### 1. Introduction

[2] Several dynamical responses to increased greenhouse gasses (GHGs) have been identified. These include an increase in the dry static stability [Frierson, 2006]; an increase in the tropopause height [Lorenz and DeWeaver, 2007]; and a poleward shift of the mid-latitude jet streams and storm tracks [e.g., Meehl *et al.*, 2007b, and references therein], which is also associated with the expansion of the tropics [Lu *et al.*, 2008]. Here we show that another robust dynamical response to increasing GHGs is an increase in the eddy length scale. The cause remains uncertain, but it appears to be linked to the increase in dry static stability.

[3] In the mid-latitudes the tropospheric circulation is dominated by eddies, which are born primarily of baroclinic instability. A fundamental characteristic of these eddies is the horizontal length scale. For a given background flow, the length scale affects both the height and the latitude at which the eddies dissipate. The location of eddy genesis and dissipation is of first order importance in determining the

time-mean atmospheric circulation [Holton, 1992; Vallis, 2006].

[4] The dynamics that determine the dominant eddy length scales is a matter of ongoing research. In so far as linear theory applies, the fastest-growing normal mode will dominate. In the Eady model the relevant measure is the Rossby radius,  $L_R = NH/f$  where  $N$  is the buoyancy frequency,  $H$  a scale height, and  $f$  the Coriolis parameter. Inclusion of a planetary vorticity gradient ( $\beta$ ) as in the Charney model makes the linear problem less tractable, but if the deep Charney mode is relevant then again a length scale that arises is  $L_R$ . However, if the flow is nonlinear then there may be a transfer of energy to larger scales, which can be arrested by  $\beta$ , friction, or a combination of the two [Rhines, 1975; Vallis and Maltrud, 1993]. If the  $\beta$  effect were of primary importance then the Rhines scale,  $L_\beta = \sqrt{U'/\beta}$  where  $U'$  is the RMS eddy velocity, might be expected to determine the eddy scale. However, in the Earth's atmosphere this scale is not significantly larger than the deformation radius  $L_R$ , and certainly no well-developed inverse cascade exists. Whether the dominant eddy length-scale is primarily determined by the Rhines scale, the deformation scale, or some combination or other factors entirely remains an open question [Vallis, 2006]. For example, using a dry primitive equation model [Schneider and Walker, 2006] found that  $L_\beta$  and  $L_R$  essentially scale in the same way as parameters vary, whereas Thuburn and Craig [1997] and Frierson *et al.* [2006] found that  $L_\beta$  was a better fit for moist primitive equation models.

### 2. Data and Methods

[5] Output from global circulation models (GCMs) used in the World Climate Research Programme's (WCRP's) Coupled Model Intercomparison Project phase 3 (CMIP3) multi-model dataset [Meehl *et al.*, 2007a] is used. We analyse the A2 ('business as usual') scenario, as this gives the largest signal to noise ratio. All models that archived both daily-mean wind-speed and monthly-mean temperature for the A2 future and 20C3M control run, are presented. This gave 12 separate models, the names of which can be found in Figures 1 and 2. Data from the NCEP/NCAR reanalysis project [Kalnay *et al.*, 1996] for 1979–2007 is also utilized.

[6] To quantify the eddy length scale, the daily meridional wind-speed ( $v$ ) was decomposed into Fourier components around latitude circles, after applying a 5th order Butterworth high-pass filter with a 30-day cutoff. The results are not sensitive to frequency filtering. The magnitude of the meridional component of the eddy kinetic energy (EKE) of an individual Fourier component at a latitude ( $\phi$ )

<sup>1</sup>Atmosphere and Ocean Science Program, Princeton University, Princeton, New Jersey, USA.

<sup>2</sup>NOAA/Geophysical Fluid Dynamics Laboratory, Princeton University, Princeton, New Jersey, USA.

<sup>3</sup>Formerly at National Institute of Water and Atmospheric Research, Auckland, New Zealand.

<sup>4</sup>Formerly at School of Geography, Environment, and Earth Science, Victoria University of Wellington, Wellington, New Zealand.

<sup>5</sup>National Institute of Water and Atmospheric Research, Auckland, New Zealand.

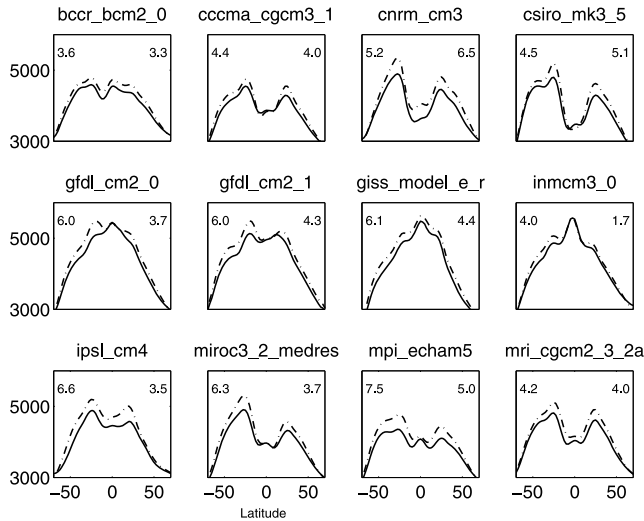


**Figure 1.** The eddy length scale at 300 hPa for the 20C3M simulation during 1981–2000 (solid line) and the A2 simulation during 2081–2100 (dashed line) for twelve of the models submitted to the Coupled Model Intercomparison Phase 3 project. See text for details of the calculation of the eddy length scale. Also shown is the percentage change in the eddy length scale between 30° and 70° latitude ( $\Delta\lambda$ ) for each hemisphere; see text for details of the calculation.

and zonal wavenumber ( $k$ ) is  $|\tilde{v}(\phi, k)|^2$ . The mean  $k$  at each  $\phi$  was calculated as

$$\bar{k}(\phi) = \frac{\sum_k k * |\tilde{v}(k)|^2}{\sum_k |\tilde{v}(k)|^2}$$

and the mean wavelength, or eddy length scale, is then  $\bar{\lambda}(\phi) = 2\pi a \cos(\phi) / \bar{k}$ , where  $a$  is the Earth's radius.

[7] The buoyancy frequency between 850 and 600 hPa is used to quantify the dry static stability, and is calculated as  $N = \sqrt{g \partial \ln(\theta) / \partial z}$  where  $g$  is gravity,  $\theta$  is the potential temperature, and  $z$  is height. The hydrostatic approximation was used to calculate  $N$  for model output on constant pressure levels.

### 3. Results

[8] The eddy length scale for the 20C3m control runs during 1981–2000 (solid line) and the A2 runs during 2081–2100 (dashed line) are shown in Figure 1. In each model, there is a climatological decrease in  $\bar{\lambda}$  towards the pole. There is large inter-model variability in  $\bar{\lambda}$  in the tropics, which may in part result from the fact that the EKE is much smaller in the tropics, so  $\bar{\lambda}$  is expected to be noisier. In every model, the dashed line is above the solid line throughout the mid-latitudes and in both hemispheres, indicating a robust increase in the eddy length scale. Quantifying the increase in eddy length scale is somewhat problematic. Because there is a poleward shift of the eddy activity in these models [Yin, 2005], and a climatological decrease in  $\bar{\lambda}(\phi)$  towards the pole, it is possible that a variance-weighted hemispheric average would decrease, even though there is an increase in the eddy length scale at every latitude. Because of this we estimate the increase in

length scale by simply weighting each latitude equally. The percentage change in the length scale ( $\Delta\bar{\lambda}$ ) is then simply the mean of  $\frac{\bar{k}(\phi)^{20C3M}}{\bar{k}(\phi)^{A2}} - 1$  between 30 and 70 degrees latitude in each hemisphere, where the superscripts distinguish the different periods.

[9] There are several plausible explanations for the increase in eddy length scale.  $L_R$  may increase because the tropopause height increases with increasing GHGs [Lorenz and DeWeaver, 2007; Meehl et al., 2007b], although it is unclear whether this is the correct  $H$  to use in the calculation or  $L_R$ . Williams [2006] found that the eddy length scale in a primitive equation model was sensitive to the tropopause height.  $L_R$  is also expected to be impacted by the change in  $N$ , which increases throughout low- and mid-latitudes [Frierson, 2006].  $L_\beta$  may increase because  $U'$  increases in the CMIP3 runs [Yin, 2005].  $L_\beta$  may also increase because of the poleward shift of the jet; in all of the models presented here the mid-latitude jet and associated eddy activity shift polewards.  $\beta$  is reduced towards the pole, causing  $L_\beta$  to increase if it is calculated at the latitude of the jet, as by Frierson et al. [2006].

[10] To investigate the cause of the increase in the eddy length scale, the inter-model variability in the change in (1) the tropopause height, (2) the static stability, (3) the eddy kinetic energy, and (4) the magnitude of the poleward shift of the jet, was compared with the change in the eddy length scale. Only the change in  $N$  averaged from 30 to 70 degrees latitude ( $\Delta N$ ) was found to be correlated with  $\Delta\bar{\lambda}$ . This relationship is shown in Figure 2. In most of the models the increase in both  $\Delta N$  and  $\Delta\bar{\lambda}$  is larger in the SH than the NH. Moreover, in both hemispheres independently, there is a positive correlation between  $\Delta N$  and  $\Delta\bar{\lambda}$ . In the Southern Hemisphere the p-value of 0.01 indicates that the correlation is significant at the 99% level. This is consistent with the hypothesis that the increase in  $N$  causes the increase in the eddy length scale. The increase in  $N$  may be caused by the fact that the saturation vapour pressure increases rapidly

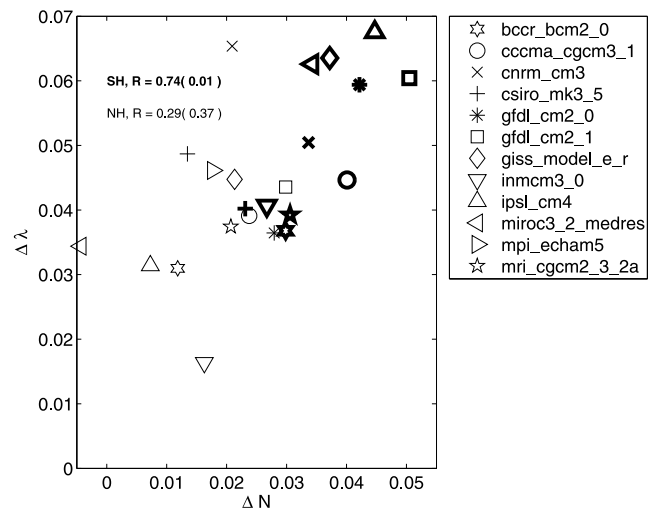


**Figure 2.**  $\Delta\bar{\lambda}$  versus the change in the mid-latitude dry static stability ( $\Delta N$ ; see text). Each point describes a single hemisphere for one model. The Northern Hemisphere is regular weight, and the Southern Hemisphere is bolded. Also shown is the linear correlation coefficient and the p-value, the likelihood of the true correlation being zero.

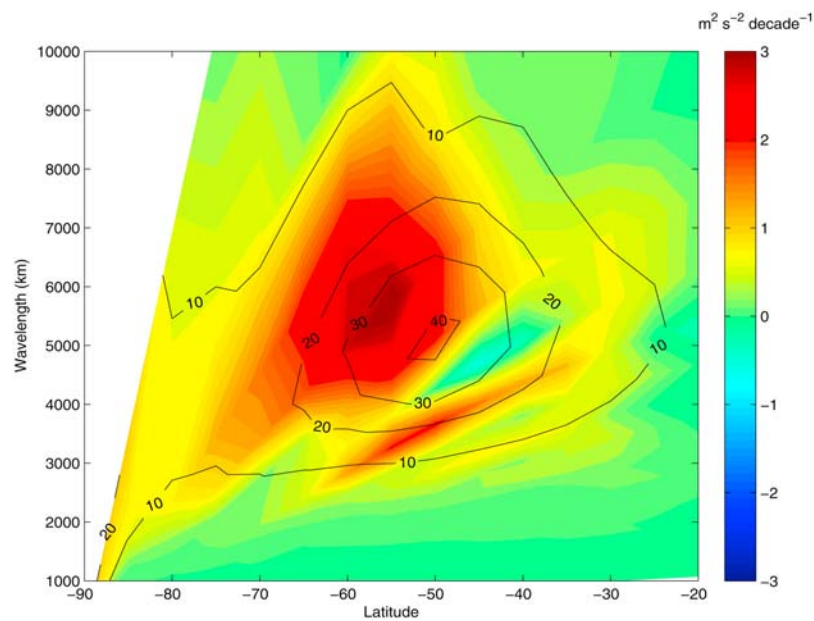


**Figure 3.** The meridional component of the eddy kinetic energy at 300 hPa in the NCEP/NCAR reanalysis data from 1979 to 2005 as a function of latitude and wavelength. See text for the details of the spectral decomposition. Contours are the climatological mean, and the shading is the linear trend.

with temperature; if relative humidity remains approximately constant, the moisture content of the atmosphere increases, and a moist adiabat has a higher dry static stability.

[11] Because the increase in the eddy length scale is a robust consequence of increasing GHGs, it might be expected that the observational data exhibit similar behaviour. Figure 3 shows the time-mean EKE at 300 hPa as a function of latitude and wavelength for the NCEP/NCAR reanalysis data. The maximum EKE occurs at 50°S and wavelengths of 3000 to 7000 km. There are three obvious features in the trends: (1) the trends are generally positive, indicative of an increase in the EKE since 1979. (2) The maximum of the trend is poleward of the climatological maximum, indicative that there has been a poleward shift of the eddy activity. This is consistent with the observation of a poleward shift in the eddy-maintained mean flow. (3) The maximum in the increase in EKE is at longer wavelengths than the time-mean maximum. This is suggestive of an increase in the eddy length scale. When  $\bar{\lambda}$  was calculated for the first and second half of the measurement period, the difference was small, but the observed changes are qualitatively similar to the projections.

#### 4. Conclusions

[12] We have shown that there is an increase in the eddy length scale in the CMIP3 model output for the future A2 scenario relative to the control. The increase is robust in that it occurs in both hemispheres in every model. The magnitude of the increase is correlated with the increase in dry static stability between 850 and 600 hPa, as would be expected if the Rossby radius is the relevant length scale for the atmosphere. In the observations, the maximum in the increase in the observed EKE in the Southern Hemisphere is at wavelengths greater than the climatological maximum, which is suggestive of an increase in the observed eddy length scale.

[13] The increase in the eddy length scale is expected to have important ramifications, and these are the subject of ongoing work. For example, because the location of the critical latitudes and associated eddy dissipation is influenced by the length scale, it is possible that the increase contributes to the poleward shift of the mid-latitude jet streams. Furthermore, because longer waves are better able to propagate into the stratosphere, they may contribute to the increase in the Brewer-Dobson overturning.

[14] **Acknowledgments.** We thank Isaac Held and three anonymous reviewers for helpful comments on previous versions of this manuscript. J. Kidston and G. K. Vallis were partially supported by NOAA grant NA07OAR4310320.

#### References

- Frierson, D. M. W. (2006), Robust increases in midlatitude static stability in simulations of global warming, *Geophys. Res. Lett.*, *33*, L24816, doi:10.1029/2006GL027504.
- Frierson, D. M. W., I. M. Held, and P. Zurita-Gotor (2006), A gray-radiation aquaplanet moist GCM. Part I: Static stability and eddy scale, *J. Atmos. Sci.*, *63*, 2548–2566.
- Holton, J. (1992), *An Introduction to Dynamic Meteorology*, Academic, San Diego, Calif.
- Kalnay, E., et al. (1996), The NCEP/NCAR 40-year reanalysis project, *Bull. Am. Meteorol. Soc.*, *77*, 437–471.
- Lorenz, D. J., and E. T. DeWeaver (2007), Tropopause height and zonal wind response to global warming in the IPCC scenario integrations, *J. Geophys. Res.*, *112*, D10119, doi:10.1029/2006JD008087.
- Lu, J., G. Chen, and D. M. W. Frierson (2008), Response of the zonal mean atmospheric circulation to El Niño versus global warming, *J. Clim.*, *21*, 5835–5851.
- Meehl, G. A., C. Covey, T. Delworth, M. Latif, B. McAvaney, J. F. B. Mitchell, R. J. Stouffer, and K. E. Taylor (2007a), The WCRP CMIP3 multi-model dataset: A new era in climate change research, *Bull. Am. Meteorol. Soc.*, *88*, 1383–1394.
- Meehl, G. T. S., et al. (2007b), Global climate projections, in *Climate Change 2007: The Physical Science Basis. Contribution of Working Group I to the Fourth Assessment Report of the Intergovernmental Panel on Climate Change*, edited by S. Solomon et al., pp. 747–845, Cambridge Univ. Press, Cambridge, U. K.
- Rhines, P. (1975), Waves and turbulence on a beta-plane, *J. Fluid Mech.*, *69*, 417–443.

- Schneider, T., and C. C. Walker (2006), Self-organization of atmospheric macroturbulence into critical states of weak nonlinear eddy-eddy interactions, *J. Atmos. Sci.*, *63*, 1569–1586.
- Thuburn, J., and G. C. Craig (1997), GCM tests of theories for the height of the tropopause, *J. Atmos. Sci.*, *54*, 869–882.
- Vallis, G. K. (2006), *Atmospheric and Oceanic Fluid Dynamics: Fundamentals and Large-Scale Circulation*, Cambridge Univ. Press, Cambridge, U. K.
- Vallis, G. K., and M. E. Maltrud (1993), Generation of mean flows and jets on a beta plane and over topography, *J. Phys. Oceanogr.*, *23*, 1346–1362.
- Williams, G. P. (2006), Circulation sensitivity to tropopause height, *J. Atmos. Sci.*, *63*, 1954–1961.
- Yin, J. H. (2005), A consistent poleward shift of the storm tracks in simulations of 21st century climate, *Geophys. Res. Lett.*, *32*, L18701, doi:10.1029/2005GL023684.
- 
- S. M. Dean and J. A. Renwick, National Institute of Water and Atmospheric Research, Private Bag 14901, Kilbirnie, Wellington 6022, New Zealand.
- J. Kidston, Atmosphere and Ocean Science Program, Princeton University, Princeton, NJ 08544, USA. (joseph.kidston@noaa.gov)
- G. K. Vallis, NOAA/Geophysical Fluid Dynamics Laboratory, P.O. Box 308, Forrester Campus, Princeton, NJ 08542, USA.